Electronic Supplementary Information (ESI)

Blue-Shifted Aggregation-Induced Emission of Siloles by Simple Structural Modification and Their Application as Nitro Explosive Chemosensor

*Jiwon Lee, Yoona Park, Joori Jung and Won-Sik Han**

Department of Chemistry, Seoul Women's University, Seoul 01797, South Korea.

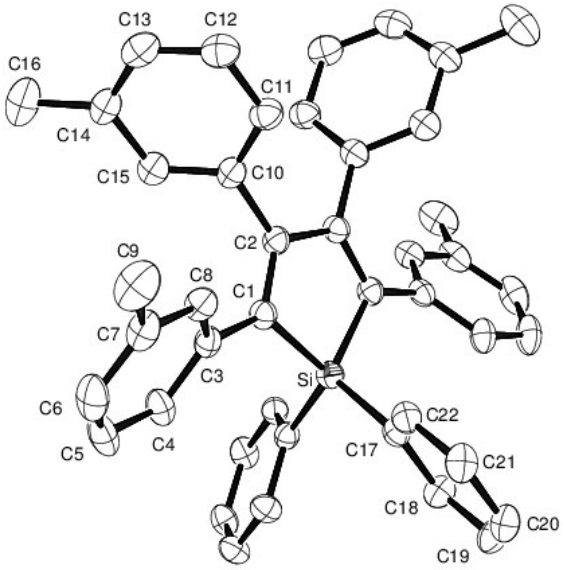

Figure S1. ORTEP structure of ***m*-TS** showing thermal ellipsoids; the probability level of this structure is 30%. Hydrogen atoms were omitted for clarity.

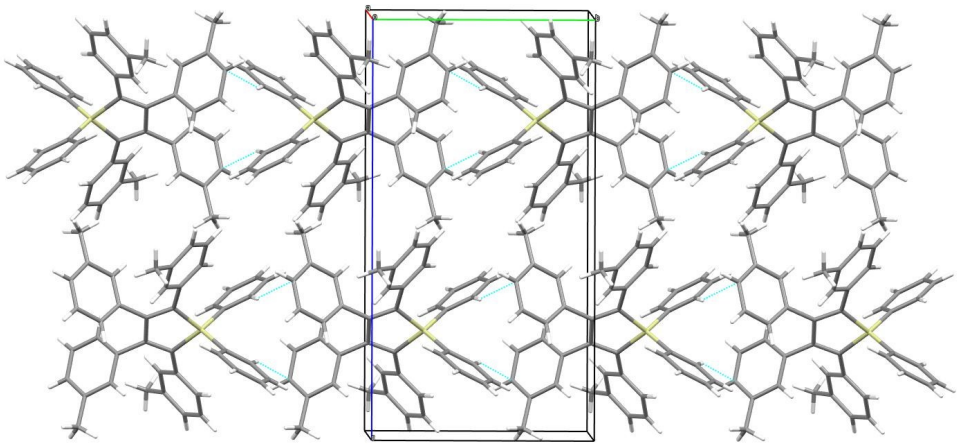

Figure S2. Crystal packing structure of ***m*-TS**.

Table S1. Crystal data and structure refinement for *m*-TS

Identification code	***m*-TS**
Empirical formula	C_{44} H_{38} Si
Formula weight	594.83
Temperature	233(2) K
Wavelength	0.71073 Å
Crystal system, space group	Monoclinic, $P2_1/c$
Unit cell dimensions	a = 8.6135(7) Å
	b = 10.2226(8) Å β = 93.739(2)°
	c = 19.2641(15) Å
Volume	1692.6(2) Å^3
Z, Calculated density	2, 1.167 Mg/m^3
Absorption coefficient, μ	0.099 mm^{-1}
F(000)	632
Crystal size	0.17 × 0.11 × 0.07 mm
θ range for data collection	1.99 to 28.30°
Limiting indices	$-11 \le h \le 11$, $-13 \le k \le 13$, $-25 \le l \le 25$
Reflections collected / unique	17009 / 4210 [R_{int} = 0.0636]
Completeness to θ = 28.40	99.8%
Refinement method	Full-matrix least-squares on F^2
Data / restraints / parameters	4210 / 0 / 207
Goodness-of-fit on F^2	1.038
Final R indices [$I>2\sigma(I)$]	$R_1{}^a$ = 0.0595, $wR_2{}^b$ = 0.1397
R indices (all data)	$R_1{}^a$ = 0.1499, $wR_2{}^b$ = 0.1981
Largest diff. peak and hole	0.424 and −0.251 e. $R_1{}^a$

$^aR_1 = \sum||F_o|-|F_c||$ (based on reflections with $F_o^2>2\sigma F^2$), $^bwR_2 = [\sum[w(F_o^2-F_c^2)^2]/\sum[w(F_o^2)^2]]^{1/2}$; $w = 1/[\sigma^2(F_o^2)+(0.095P)^2]$; $P = [\max(F_o^2, 0) + 2F_c^2]/3$(also with $F_o^2>2\sigma F^2$.

Table S2. Bond lengths [Å] for *m*-TS

Si-C(17)#1	1.866(3)	C(7)-C(9)	1.508(5)
Si-C(17)	1.866(3)	C(10)-C(15)	1.383(4)
Si-C(1)#1	1.877(3)	C(10)-C(11)	1.388(4)
Si-C(1)	1.877(3)	C(11)-C(12)	1.394(4)
C(1)-C(2)	1.361(4)	C(12)-C(13)	1.361(5)
C(1)-C(3)	1.482(4)	C(13)-C(14)	1.369(5)
C(2)-C(10)	1.500(4)	C(14)-C(15)	1.419(4)
C(2)-C(2)#1	1.504(5)	C(14)-C(16)	1.489(5)
C(3)-C(4)	1.393(4)	C(17)-C(22)	1.395(4)
C(3)-C(8)	1.393(4)	C(17)-C(18)	1.399(4)
C(4)-C(5)	1.386(4)	C(18)-C(19)	1.378(4)
C(5)-C(6)	1.370(5)	C(19)-C(20)	1.377(4)
C(6)-C(7)	1.388(5)	C(20)-C(21)	1.371(4)
C(7)-C(8)	1.393(4)	C(21)-C(22)	1.389(4)

Table S3. Angles [°] for *m*-TS

C(17)#1-Si-C(17)	110.14(18)	C(8)-C(7)-C(9)	120.4(4)
C(17)#1-Si-C(1)#1	110.46(13)	C(7)-C(8)-C(3)	122.5(3)
C(17)-Si-C(1)#1	116.47(12)	C(15)-C(10)-C(11)	119.1(3)
C(17)#1-Si-C(1)	116.47(12)	C(15)-C(10)-C(2)	119.2(3)
C(17)-Si-C(1)	110.45(13)	C(11)-C(10)-C(2)	121.6(3)
C(1)#1-Si-C(1)	92.04(18)	C(10)-C(11)-C(12)	120.3(3)
C(2)-C(1)-C(3)	125.3(3)	C(13)-C(12)-C(11)	119.0(4)
C(2)-C(1)-Si	107.9(2)	C(12)-C(13)-C(14)	123.6(3)
C(3)-C(1)-Si	126.5(2)	C(13)-C(14)-C(15)	116.7(3)
C(1)-C(2)-C(10)	123.2(2)	C(13)-C(14)-C(16)	123.5(3)
C(1)-C(2)-C(2)#1	116.07(16)	C(15)-C(14)-C(16)	119.7(4)
C(10)-C(2)-C(2)#1	120.75(15)	C(10)-C(15)-C(14)	121.2(3)
C(4)-C(3)-C(8)	118.0(3)	C(22)-C(17)-C(18)	116.8(3)
C(4)-C(3)-C(1)	119.8(3)	C(22)-C(17)-Si	121.6(2)
C(8)-C(3)-C(1)	122.2(3)	C(18)-C(17)-Si	121.6(2)
C(5)-C(4)-C(3)	119.9(3)	C(19)-C(18)-C(17)	121.8(3)
C(6)-C(5)-C(4)	120.9(4)	C(20)-C(19)-C(18)	119.9(3)
C(5)-C(6)-C(7)	120.9(3)	C(21)-C(20)-C(19)	120.1(3)
C(6)-C(7)-C(8)	117.7(3)	C(20)-C(21)-C(22)	120.1(3)
C(6)-C(7)-C(9)	121.9(3)	C(21)-C(22)-C(17)	121.3(3)

Table S4. Dihedral angles [°] for *m*-TS

C(17)#1-Si-C(1)-C(2)	-114.1(2)	C(1)-C(2)-C(10)-C(11)	113.3(4)
C(17)-Si-C(1)-C(2)	119.3(2)	C(2)#1-C(2)-C(10)-C(11)	-67.0(5)
C(1)#1-Si-C(1)-C(2)	0.03(15)	C(15)-C(10)-C(11)-C(12)	1.9(5)
C(17)#1-Si-C(1)-C(3)	71.5(3)	C(2)-C(10)-C(11)-C(12)	-174.5(3)
C(17)-Si-C(1)-C(3)	-55.1(3)	C(10)-C(11)-C(12)-C(13)	-1.6(5)
C(1)#1-Si-C(1)-C(3)	-174.4(3)	C(11)-C(12)-C(13)-C(14)	-0.3(5)
C(3)-C(1)-C(2)-C(10)	-5.9(5)	C(12)-C(13)-C(14)-C(15)	1.8(5)
Si-C(1)-C(2)-C(10)	179.6(2)	C(12)-C(13)-C(14)-C(16)	-175.9(3)
C(3)-C(1)-C(2)-C(2)#1	174.4(3)	C(11)-C(10)-C(15)-C(14)	-0.4(4)
Si-C(1)-C(2)-C(2)#1	-0.1(4)	C(2)-C(10)-C(15)-C(14)	176.1(3)
C(2)-C(1)-C(3)-C(4)	138.5(3)	C(13)-C(14)-C(15)-C(10)	-1.4(4)
Si-C(1)-C(3)-C(4)	-48.0(4)	C(16)-C(14)-C(15)-C(10)	176.4(3)
C(2)-C(1)-C(3)-C(8)	-43.1(4)	C(17)#1-Si-C(17)-C(22)	-143.5(3)
Si-C(1)-C(3)-C(8)	130.4(3)	C(1)#1-Si-C(17)-C(22)	89.7(3)
C(8)-C(3)-C(4)-C(5)	3.1(5)	C(1)-Si-C(17)-C(22)	-13.5(3)
C(1)-C(3)-C(4)-C(5)	-178.4(3)	C(17)#1-Si-C(17)-C(18)	36.7(2)
C(3)-C(4)-C(5)-C(6)	-1.6(5)	C(1)#1-Si-C(17)-C(18)	-90.0(3)
C(4)-C(5)-C(6)-C(7)	-1.1(6)	C(1)-Si-C(17)-C(18)	166.8(2)
C(5)-C(6)-C(7)-C(8)	2.1(5)	C(22)-C(17)-C(18)-C(19)	-1.1(4)
C(5)-C(6)-C(7)-C(9)	-176.9(3)	Si-C(17)-C(18)-C(19)	178.6(2)
C(6)-C(7)-C(8)-C(3)	-0.5(5)	C(17)-C(18)-C(19)-C(20)	0.8(5)
C(9)-C(7)-C(8)-C(3)	178.5(3)	C(18)-C(19)-C(20)-C(21)	0.0(5)
C(4)-C(3)-C(8)-C(7)	-2.1(5)	C(19)-C(20)-C(21)-C(22)	-0.4(5)
C(1)-C(3)-C(8)-C(7)	179.5(3)	C(20)-C(21)-C(22)-C(17)	0.1(5)
C(1)-C(2)-C(10)-C(15)	-63.2(4)	C(18)-C(17)-C(22)-C(21)	0.7(4)
C(2)#1-C(2)-C(10)-C(15)	116.5(4)	Si-C(17)-C(22)-C(21)	-179.0(2)

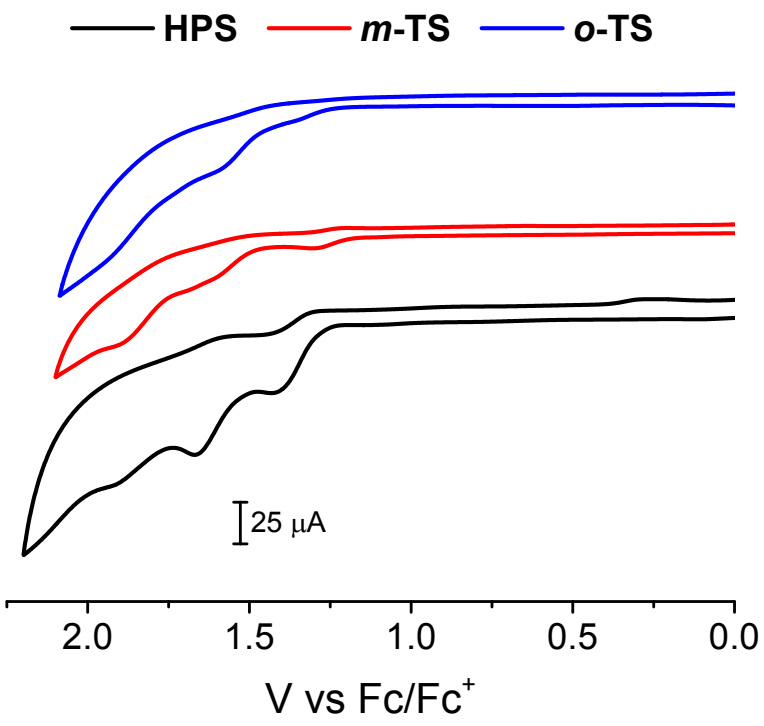

Figure S3. Cyclic voltammograms of **HPS**, ***m*-TS**, and ***o*-TS** in dichloromethane solution containing 0.1 M *n*-Bu_4NPF_6 as electrolyte, at a scan rate of 0.1 V s^{-1}.

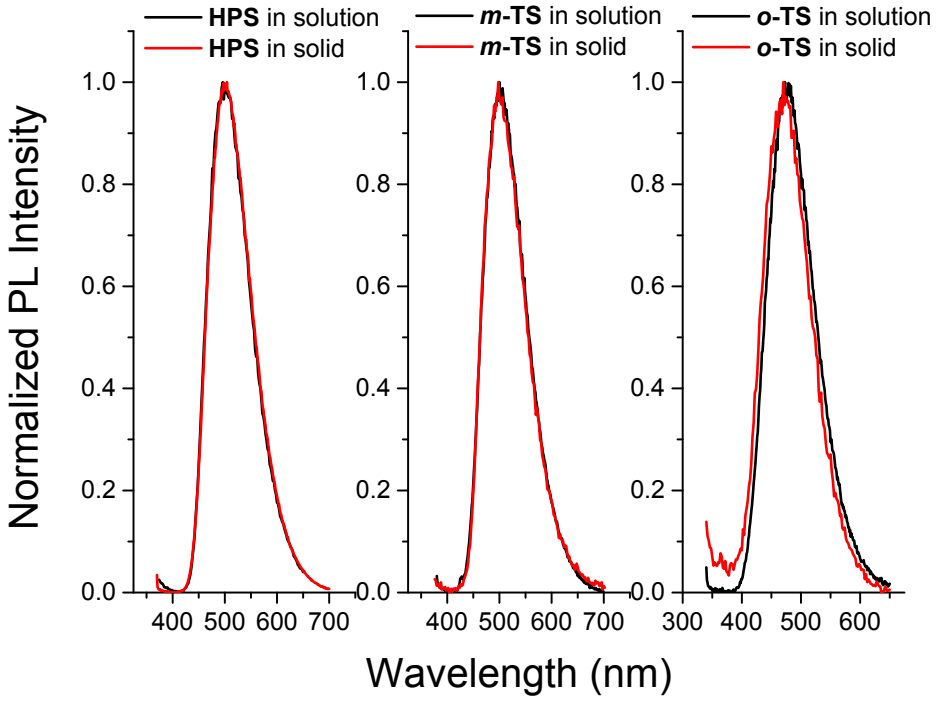

Figure S4. Photoluminescence spectra of **HPS**, ***m*-TS**, and ***o*-TS** in acetone/water (f_w = 90%) and solid-state thin layers absorbed on the TLC plates.

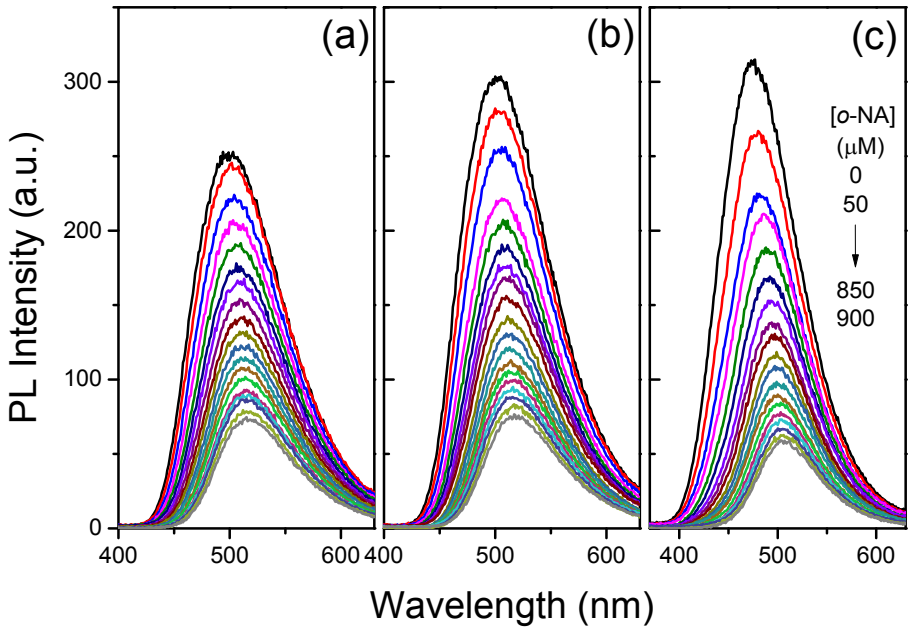

Figure S5. Decrement of emission intensities of (a) **HPS**, (b) ***m*-TS**, and (c) ***o*-TS** in acetone/water mixtures by *o*-nitroaniline (*o*-NA) (concentration: 10 μM and excited at 320 nm).